



ELSEVIER

Colloids and Surfaces A: Physicochem. Eng. Aspects xxx (2005) xxx–xxx

COLLOIDS
AND
SURFACES

A

www.elsevier.com/locate/colsurfa

Differences between protein and surfactant foams: Microscopic properties, stability and coarsening

A. Saint-Jalmes*, M.-L. Peugeot, H. Ferraz, D. Langevin

Laboratoire de Physique des Solides, Université Paris-Sud, 91405 Orsay, France

Received 3 November 2004; received in revised form 2 February 2005; accepted 8 February 2005

Abstract

We report results on foamability, stability and coarsening of foams made either of surfactant (SDS) or of milk protein (casein) solutions. Studies have been performed at the scales of the gas–liquid interface, thin liquid film and bubble size, in order to find the correlations between these different scales, and to elucidate the microscopic origins of the macroscopic features. For both systems, foamability concentration thresholds have been measured, and a bubble size dependence has been found. A clear correlation between the stability of an isolated thin film and the foam stability is always evidenced. However, the mechanism of stability of the casein thin films is different from the surfactant one, and related to the confinement and percolation of casein aggregates. We also report results on coarsening at constant liquid fraction, showing that the protein foams coarsen more slowly than the surfactant ones, and that it is due to differences in thin film thickness.

© 2005 Elsevier B.V. All rights reserved.

Keywords: Foam; Stability; Coarsening; Surface tension; Thin film; Protein

1. Introduction

Aqueous foams are familiarly stabilized by small soap molecules (surfactant), when they are used in the field of detergency, cleaning etc. [1,2]. Oppositely, for the food-related applications, foams are mostly stabilized by protein molecules [1]. In spite of their wide use in food products, the stabilization mechanisms are not yet completely known for these protein foams, as well as the conditions required for good foaming (or foamability). For small surfactants, the properties at liquid interfaces or in bulk, together with the thin liquid films properties are well known, and the relations with the mechanism of foaming and stability have been identified. It is known that surfactants make micelles in bulk above the critical micellar concentration (cmc), and that above this cmc the interfaces are saturated in surfactants [1]. The cmc is then often used as a simple concentration criterion for foamability. Then, for most of the classical surfactants (which are charged molecules), the stability of the thin films and of the

foam, is due to the electrostatic repulsion between the surfactant covered bubble surfaces, resulting in high disjoining pressures [3,4]. In comparison with the knowledge on surfactants, much less is known on the protein systems: it is for instance important to determine if simple criterions for foaming can be defined, if critical concentrations can be found in connection with the foaming properties, and if one can finally elucidate the main contributions of the disjoining pressure, thus explaining the origins of stability of protein foams.

Another important issue is to know if the macroscopic properties of protein and surfactant foams are different; in a more general way, to find out how much the foam properties depend on the chemicals used. Some results are already known: concerning drainage, it has been found that the chemicals are important via the surface shear viscosity [5,6]. Proteins adsorbed at interfaces create highly viscoelastic layers [7–10], with high surface shear viscosities, resulting in very rigid Plateau Borders boundaries, whereas the opposite is usually found for pure surfactant foams [2,5,6]. Regarding the macroscopic foam mechanical properties, beside the simple dependence with the surface tension, it has also been found that the viscoelasticity depends in a more complex manner on

* Corresponding author. Tel.: +33 1 69 15 6960; fax: +33 1 69 15 6086.
E-mail address: saint-jalmes@lps.u-psud.fr (A. Saint-Jalmes).

the chemicals used, and this remains to be completely understood [11,12]. The tricky point is always to figure out which microscopic parameters control the macroscopic properties. The role of the chemicals adsorbed at the interfaces is even more unknown for problems like coarsening or coalescence, while recent works suggest that the interfacial viscoelastic properties may influence the coarsening process [13,14].

In this article, in order to answer some of these issues, we have selected and studied two opposite systems: a surfactant (SDS) and a protein (casein) solutions. We present results obtained at the different length scales of a foam, from the smallest one of the gas–liquid interface to the macroscopic scale, where foaming and coarsening are studied. This allows us to investigate and find some correlations between the properties at all these different scales.

2. Materials and methods

The two widely used surface active compounds studied here are: the milk casein (CAS), and the surfactant sodium dodecyl sulfate (SDS), both purchased from Sigma. The casein powder contains all the milk caseins (α , β and κ). The β -casein (30% of all the milk proteins) is the most surface active, often considered as a natural flexible diblock copolymer (209 amino acids residues, $M_w = 24$ kDa). In solutions, even at low concentrations, most of the caseins exist in a colloidal particle, the so-called micelle, with typical diameters varying from 50 to 300 nm. Though the micelle structure is not yet completely understood, it is supposed to be made of sub-units (sub-micelles) linked by calcium and magnesium ions. The sub-micelles contain between 10 and 100 casein molecules, with typical size from 10 to 25 nm. In our studies, the casein concentrations are varied from 0.03 to 1 g/L, solutions are sonicated to ensure good dissolution, pH is set at 5.6 by a phosphate buffer, and only “fresh” solutions are used (within the first 2 days). SDS is used as received (purity > 99%), and concentrations from 0.05 to 5 g/L were studied.

We have used a simple setup for the foamability tests. At the bottom of a long Plexiglas column, some air is blown at controlled rates into the solution, through calibrated glass frits or nozzles (in order to control and change the bubble size). The foam volume V_f is measured as a function of time, and compared to the amount of gas injected V_g . In a steady state, after a few minutes, the ratio $K = V_f/V_g$ becomes independent of time: a good foamability will correspond to $K \approx 1$, while poor foamability to $K \ll 1$. Starting from very low values and increasing the concentrations of surface active compounds, the coefficient K rises from 0 to close to 1. We then define a foamability concentration threshold c_s by $K(c_s) = 0.5$.

A second foam production method is used for the coarsening studies. The foam are produced by a turbulent mixing method, which creates foam with an initial mean bubble diameter $d_0 \approx 120 \mu\text{m}$ [15]. In order to study coarsening without drainage, we have developed a rotating cell setup. The cell remains fixed during a time period τ , after which it is rapidly

rotated upside down, inverting the drainage direction. The cell size and the period τ are optimized to obtain a constant liquid fraction ε for long period of times at the cell center. The cell is 40 cm high, 12.5 cm wide and 2.5 cm thick, and is made of transparent Plexiglas. The period τ is between 20 and 200 s depending of the foam used (different gas and liquid fractions). Note that with time, τ must be reduced as bubbles get larger, and drainage is faster. Here, an important parameter, making the experiment feasible, is the initial bubble size: drainage is indeed very slow for foams with $d_0 \approx 120 \mu\text{m}$, whereas the coarsening is quite fast. In fact, a typical ratio R of the drainage time over the coarsening one scales like d_0^4 [16], and here $R \ll 1$. The evolution of the bubble size $d(t)$ is followed by light transmission: in the limit of multiple scattering, the transmitted intensity by a foam, I_t , depends both directly on d , and in a more complex way on the liquid fraction ε [17]. So for a fixed liquid fraction, one can obtain the variations of d directly from those of I_t . In practice, a white homogeneous illumination is applied on one side of the cell, and a CCD camera collect the intensity on the other side. Theoretically, coarsening is predicted to be a self-similar process [18,19], to which corresponds a growth law for the bubble diameter mean value $d(t)$: $d(t)^2 - d_0^2 = d_0^2(t - t_0)/t_c$ (d_0 is the initial mean bubble diameter, at $t = t_0$). In the asymptotic limit of long times, a simple scaling is expected, $d \sim t^{1/2}$, which has been experimentally reported [20]. The characteristic coarsening time is given by $t_c = (d_0^2 h)/(2K_{\text{geo}}K_{\text{gas}}\gamma f(\varepsilon))$, with K_{geo} is a geometrical constant (reflecting the bubble geometry), K_{gas} a gas constant (including the diffusivity and solubility constant), $f(\varepsilon)$ a function of the liquid content, h the thin film thickness, and γ is the surface tension [16,21].

The thin film balance is used for investigating the stability and the properties of single foam film [3,4]. In this technique, the film is created and held on a horizontal support (a glass frit filled with solution, mimicking the Plateau borders around the real foam film). In the usual setup, external pressures are applied over the film, corresponding to different disjoining pressures π and resulting in different equilibrium thickness h (measured by interferometry). Together with the $\pi(h)$ curve, important information are also obtain by the direct observation of the film uniformity and morphology (monitored by videomicroscopy). Here, regarding stability issues, rather than studying π as a function of h , we have simply applied single sharp steps of over pressures (from 0 to a few hundred of Pa), and check how the film behaves, thins, and if it resists or breaks. This situation is chosen to mimic the collision and packing of two bubbles in a real foam. In our setup, the diameter of the hole in the frit is 1.4 mm; this thus corresponds to the bubble face diameter, and then to a bubble diameter of typically 3 mm.

At the scale of the gas–liquid interface, we have studied the time evolution of the surface tension (often called “dynamic surface tension”) both by the maximum bubble pressure, and pendent drop methods. With the first method, bubbles are formed at the tip of a capillary: the maximum pressure applied to create a bubble corresponds to a bubble radius equal to the

one of the capillary, and it is then possible to extract the surface tension via the Laplace equation. This technique is especially well-suited for the very short times range (down to ms). In the second technique, the surface tension is deduced from the droplet (or bubble) shape, pending (or rising) at the tip of a syringe (oriented downward or upward) [1].

3. Results

3.1. Foamability

Fig. 1 shows typical data found with the foamability setup. The height of foam in the column is plotted as a function of time, for different casein concentrations c (fixed bubble size). The arrow indicates the increase of the concentrations. At low c , almost no foam is produced, and the coefficient K is ≈ 0.1 . This corresponds to many bubble ruptures, with most of the injected gas not being actually incorporated in the foam. For the highest concentrations, the curve becomes linear, and the amount of foam (at any given time) becomes almost independent of c . In that regime, the foaming is optimal and all the gas is entrapped into the foam ($K \approx 0.9$, also meaning that the foams produced are rather dry). With casein solutions, and for any bubble sizes, the curve $K(c)$ presents a well-defined range of concentration where K rises from 0.1 to 0.9 (S-shape curve), meaning that there is really a threshold in concentration for foamability. Thus, defining a single threshold concentration c_s (with $K(c_s) = 0.5$) appears meaningful. Our results on casein solutions show that c_s strongly depends on the bubble size, but not on the injected gas flow rate (typically varied from 0.1 to 1 L/min). Same trends have been found while performing the measurements with SDS, where it is also easy to determine a concentration threshold c_s . The dependence of c_s with bubble size is reported in Fig. 2: both for casein and SDS, it is found that c_s increases with d , and in the range investigated here, the dependence is somehow linear (with $c_s(\text{SDS}) > c_s(\text{CAS})$). Note that for SDS we

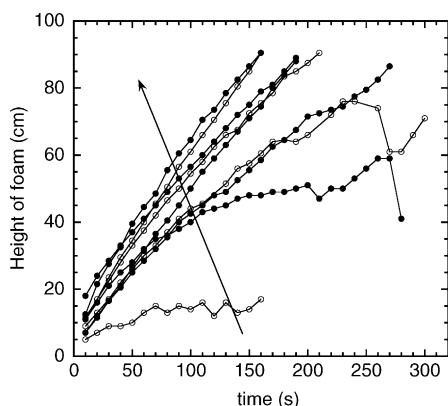


Fig. 1. Foamability measurements: foam height as a function of time, for different casein concentrations, and with a fixed bubble size $d = 1.5$ mm. The arrow indicates the increase of concentration. The cross-section of the cell is 4 cm \times 4 cm.

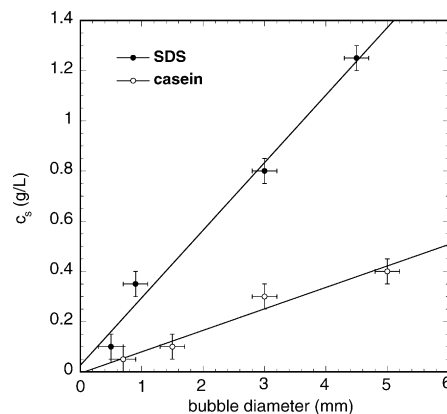


Fig. 2. Foamability concentration threshold c_s (as defined in the text) for different bubbles sizes, for SDS and casein.

have found that c_s is always a few times lower than the cmc (2.8 g/L). For casein, a typical mean value of c_s is 0.2 g/L, and one has now to figure out from which microscopic parameters and stabilization mechanism this typical value emerges.

Preliminary experiments on SDS/casein mixtures show that these solutions have unexpectedly high foamability. The mixtures actually foam better than what could be expected from the foaming of each solution taken separately, possibly evidencing some synergistic effects. This remains to be studied in a systematic and detailed way, and it is an ongoing work.

3.2. Coarsening at constant liquid fraction

With casein and SDS concentrations well above the foamability threshold ($c(\text{SDS}) = 8$ g/L, and $c(\text{CAS}) = 5$ g/L), stable foams are obtained for the coarsening studies. For the gas, we used either N_2 or perfluorohexane C_2F_6 . With the latter, one obtains low coarsening rates, meaning also low drainage rates [16–21,22], with which the measurements are easier to perform, but providing less bubble size variations. Fig. 3 shows

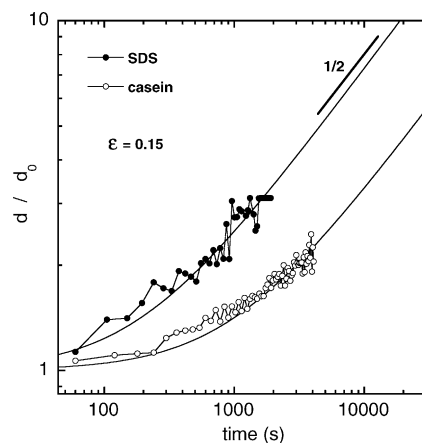


Fig. 3. Relative bubble size evolution with time measured by light transmission, at constant liquid fraction $\epsilon = 0.15$, with initial bubble size $d_0 = 120$ μm . The lines correspond to the model described in the text.

the results obtained for the time evolution of d/d_0 for casein and SDS foams, both at a constant liquid fraction $\varepsilon = 0.15$, with almost equal d_0 (with casein, the mean bubble diameter is slightly smaller than for SDS) and made of N_2 . Both data set can be fitted by the predicted law (solid line) described previously. However, we found that the corresponding t_c are different: $t_c(\text{casein}) = 980$ s and $t_c(\text{SDS}) = 190$ s (so that $t_c(\text{casein})/t_c(\text{SDS}) \approx 5$). The coarsening rate is thus significantly smaller for the casein foams, at a fixed liquid fraction and bubble size. A similar ratio for t_c was found with C_2F_6 , showing that this effect is independent of the gas: $t_c(\text{casein}) = 19100$ s and $t_c(\text{SDS}) = 4200$ s.

3.3. Surface tension

As the adsorption of the surfactants or of the caseins proceeds at the air–liquid interface, its surface tension decreases. For surfactants, at any given concentrations, an equilibrium is usually obtained within the first minute. For casein (as for most proteins) the adsorption is much slower, and the dynamics strongly depends on the bulk concentration. In fact, if one wants to correlate surface tension and foamability, it is important to determine a typical adsorption time, after which it is relevant to know the surface tension. As a first attempt, we have considered the time taken by a bubble between its creation on the frit and its arrival on the above foam (where it hits the other bubbles, and get jammed). It is indeed during that time that adsorption is possible. In our setup, we estimate this time to be 3 s. We have thus reported in Fig. 4 the surface tension γ as a function of the bulk concentration c , measured with the maximum bubble pressure, after 3 s (and corresponding to a bubble diameter $d \approx 1.5$ – 2 mm). Measurements with the pendent drop technique provides the same results, but with slightly less accuracy. Here again, we have found a difference between the two type of solutions. For casein, after these 3 s, almost no adsorption is detected in the range of concentration tested: the surface tension remains close to the one of pure water. For the SDS, the adsorption is much more active at these small timescales, as the surface

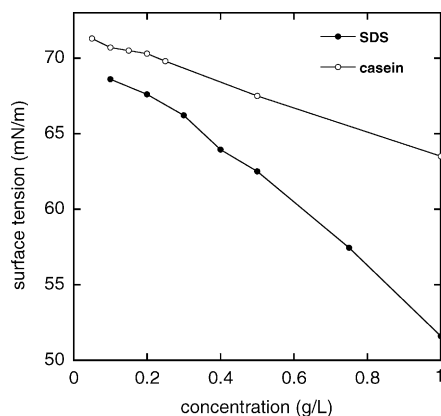


Fig. 4. Surface tensions, after 3 s, measured by the maximum bubble pressure method, as a function of the SDS and casein concentration.

tension significantly decreases with increasing the concentration.

3.4. Thin film studies

The structure, thickness and disjoining pressure curves of small surfactant, like SDS, have been extensively studied, especially with the thin film balance [3,4]. Here, for the SDS, we have recovered some classical results. Under an applied pressure step, films get formed, then always thin in a few seconds, down to very small thickness (around 10 nm). They usually remain very flat and uniform, though some dimples can be trapped in the first drainage stage (at the highest concentrations). A transition from the common black film (CBF) to the Newton black film (NBF) [3,4] is also sometimes observed, before film rupture. At the lowest concentrations ($c < 0.2$ g/L), the films are strongly unstable and break in a few seconds, and it is only for $c > 0.6$ g/L that they are getting quite stable (at least for a few minutes). At this stage, it is however indeed difficult to determine a precise concentration threshold for film stability, as it would require a complete statistical study and a large number of measurements to reduce the error bars.

Regarding the casein films, Fig. 5 represents top views of the thin films at three concentrations. One important observation is that these films are always heterogeneous in thickness with the presence of thick spots (or bumps), which density in the film depends on the bulk concentration. In Fig. 5a, with $c = 0.05$ g/L (representative of the low concentration range, $c < 0.1$ g/L), only a few thick regions are detected, while most of the film gets rapidly very thin, and eventually breaks. The sizes and thickness of these regions are respectively on the order of a few microns and hundred of nanometers. These thick spots can be interpreted as confined casein aggregates, containing probably many casein micelles, which are trapped in the films, and cannot flow. The density of aggregates, for which the thin film becomes stable typically corresponds to the image in Fig. 5b ($c = 0.3$ g/L). At that stage, it seems that the aggregates are no longer isolated from each others in the film; but on the contrary, they get connected, providing some rigid and thick bridges between the sides of the film (possibly similar to a percolation process), and a coverage of approximately 50% of the film. At the highest concentrations, the film is completely filled with aggregates and

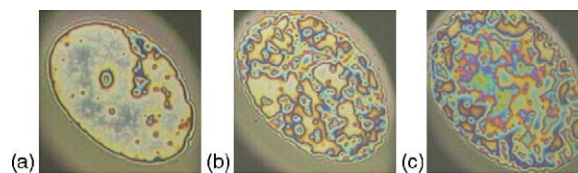


Fig. 5. Top views of casein thin films, obtained with the thin film balance apparatus, at three different casein bulk concentrations: (a) $c = 0.05$ g/L, (b) $c = 0.3$ g/L and (c) $c = 0.8$ g/L, showing the thickness heterogeneity, and the presence of thick regions (confined casein aggregates), which surface density depends on the concentration. The thin films becomes stable as soon as these confined aggregates can percolate (b).

its surface is quite corrugated. The films are then extremely stable: they almost do not thin or drain under an increased pressure, as they appear as “gelified” in all their volume. In that concentration range (Fig. 5c), the film resemble very much to those observed for mixed surfactant/polyelectrolytes films, close to the precipitation conditions [23]. The addition of SDS strongly changes the film morphology: starting with $c = 0.5$ g/L of casein, and with only a small SDS amount of 0.1 g/L added, almost all the thick regions have been removed and the films simply resemble to those of pure SDS. So it seems that the pre-adsorption of SDS prevent the confinement of the casein aggregates in the film. These results cannot be easily linked to those on the foamability of mixtures. In order to understand the 3D behavior of these foams, the structure and the composition of the mixed SDS/casein interfacial layers and thin films remain to be determined. Note finally that other studies with only pure β -casein solutions [24], or only non-aggregated sub-micelles of casein [25] have shown that the films are more homogeneous in morphology and thickness, with stepwise thinning.

4. Discussion

We can now check if the results obtained at these different length scales allow us to explain the foamability and coarsening results. It is also interesting to test if the results obtained on isolated single foam structures (interface and thin film) are consistent with the 3D behavior. First let us look at the SDS results. The typical bubble diameter d in the surface tension measurement is 1.5–2 mm, and at this size corresponds a 3D foamability threshold $c_s = 0.45$ g/L (Fig. 2). At such a c_s , it is found that some significant adsorption has actually occurred within the first 3 s (with a decrease of almost 10 mN/m when compared to pure water). As usually expected for surfactant, it appears that there are some clear connection between surfactant adsorption and foamability. However, we have already pointed that the c_s values are smaller than the cmc, here one can see how far the surface density needed for foam stability (corresponding to a surface tension of 62 mN/m) is below the maximum possible coverage (corresponding to a surface tension of 36 mN/m at the cmc). The SDS thin film studies show that the threshold of film stability, though difficult to determine, is roughly in agreement with the foamability one, and it is here also possible to make a clear connection between these two length scales. The fact that the thin films are flat and thin is indeed consistent with homogeneously covered surfaces. Moreover, when they are stable, the disjoining pressure curves can be nicely interpreted by DLVO models, for which the main repulsive contribution is an electrostatic one, corresponding to homogeneously charged surfaces [3,4]. We thus believe that, for a surfactant systems like SDS, the freshly made bubbles get first covered by surfactants, and then repulsive forces between the adsorbed surfactant layers allow (or not if the surface density is not high enough) for the stabilization of the film, and of the foam. In that sense,

both independent measurements of the dynamic surface tension and of the thin film properties appears to be very useful for foamability predictions, and the different sets of results at all the length scales are consistent. We also believe that the same stability sequence mechanism (a first rapid adsorption, then repulsion between covered surfaces) should probably be valid for most of the low molecular weight surfactant systems, like with the cationic C_n TAB (alkyltrimethylammonium bromide) for instance, as the related stable thin films are always very uniform and flat. However, one must be aware that the conditions for the thin film and foam stability (especially, in terms of concentrations) depends also on the chemistry of the molecule (length of the chain, or type of head group) [26].

Now, concerning the casein solutions, at the measured 3D foamability threshold ($c_s = 0.15$ g/L, for $d_0 = 2$ mm) the surface tension after 3 s is still close to the one of pure water, meaning almost no adsorption (and this remains true to at least $c = 3c_s$). So, following the conclusions obtained for SDS, and if one only relates on a criterion based on dynamic surface tension measurements, there should be no foam at these concentrations. On the contrary, we have found good correlations between macroscopic foamability and thin film stability: for similar bubble size ($d \approx 3$ mm), the 3D foamability threshold and the one for thin film stability are close ($c = 0.2$ – 0.3 g/L).

So, it seems that the mechanisms of stability of the casein and SDS foams are quite different. For the casein solutions, when the bubbles get in contact and packed at the bottom of a foam sample, their surfaces seem to be poorly covered (high surface tensions). But stable foams can nevertheless be produced, due to the confinement of casein aggregates between the bubbles in the thin films. These aggregates, which were not previously completely adsorbed on the surfaces finally provide the film (and the foam) stability, possibly via a percolation process. Such a percolation of the aggregates may rigidify the film, avoiding any more flow or drainage, and preventing large areas of the film to get to very low unstable thickness. Here again, it is interesting to note that this mechanism (simple confinement and percolation of aggregates, without previous adsorption) may not be relevant only for the casein solutions, but could be also valid for foams and emulsions stabilized by other high molecular weight molecules (other proteins or solid particles, for which the adsorption at a liquid interface is not fast and efficient). Note however, as for the low molecular weight surfactant systems, that we are discussing here a possible origin for the thin film stability with large molecules, but that the foamability itself of protein solutions depends obviously strongly on the protein chemistry [9].

These results also show that independent measurements of dynamic surface tension are not relevant for explaining or predicting the protein solution foamability. It may be important to note that for these surface tension measurements, the bubble is fixed and no motion occurs in the fluid; which is not the case in the real situation where the bubble is rising upwards. However, it is not clear if the motion of the

bubble can result in a different, and possibly higher, surface adsorption coverage. In fact, the duration of the bubble motion remains short (3 s), a time which remains small when compared to the typical anchoring times (time needed for a single casein to completely and definitively adsorb at the interface); moreover, it is possible that the anchoring efficiency may be actually reduced by the relative bubble motion. So, in spite of the bubble rising into the solution, the bubble surfaces are still probably widely uncovered when they finally hit each other in the foam. It would then be interesting to be able to measure the effective in situ surface tension, once the bubbles are in contact, and with the aggregates finally adsorbed.

With these results on the mechanisms of foam stabilization, we can now look at the linear dependence of the threshold concentration c_s with the bubble diameter. For a surfactant, to any given bulk concentration corresponds a single surface density (surface tension), at long times and at equilibrium. This means that, at equilibrium, surfaces are covered at the same surface density whatever their areas, avoiding then any bubble size dependence. As we have found a different behavior, a first hypothesis is that this effect is related to the dynamics of adsorption (before the equilibrium), with intermediate surface densities depending on the size of the bubble. One can also wonder if, even with equal mean surface density, bigger surface density gradients could occur for larger bubble surfaces, providing more film rupturing (and thus necessitating higher bulk concentration to avoid them). For the casein, the situation is somehow similar, and it is possible that for large bubble surfaces, big areas of very thin and unstable thickness can occur, making the films more fragile. In the same time, it is also not obvious that, for a given bulk concentration, the effective surface density of aggregates confined in the film, or even their size, is independent of the film area. Clearly, more experiments on the microscopic properties, corresponding to various bubble sizes, are needed to elucidate completely these macroscopic bubble size effects.

We can finally check if our results allow us to explain the differences in the coarsening rates. As reported before, the ratio $t_c(\text{casein})/t_c(\text{SDS}) \approx 5$. Back to the model predicting t_c , we can first check if it can explain this result. For these two experiments the liquid fraction, gas and initial bubble diameter can be considered as identical. Regarding the surface tensions, for SDS $\gamma = 36$ mN/m since the concentration is above the cmc; for the casein, we also take the value corresponding to the maximum coverage since the bulk concentration is very high, meaning that the surfaces are completely saturated of casein. In fact, at these concentrations, the initial surface tension (measured by the pendent drop technique) after a few seconds is already close to the equilibrium value at longer times, $\gamma = 42$ mN/m. So the differences between the surface tension is finally also small. In fact, our studies have shown that the only significant difference is in the thin film thickness. For the SDS films, a mean thickness (for a liquid fraction of 0.15, and at low capillary pressures) is between

30 and 40 nm, whereas a mean value can be approximated to be around 200–250 nm for the casein (Fig. 5c), so a typical thickness ratio $h(\text{casein})/h(\text{SDS}) \approx 5\text{--}7$. It is thus reasonably possible to explain the differences in coarsening rates simply by the differences in film thickness. The agreement is in fact even better if one also include the small surface tension difference. So, these results tend to prove that no new contributions coming from the viscoelastic or other interfacial properties have to be taken into account regarding the coarsening process, as it has also been found with measurements on isolated bubble covered by casein molecules [27]. Note finally that the same difference of coarsening rates between SDS and casein foams has been recovered in an indirect manner, via rheological creep experiments which provide information on the role of coarsening in macroscopic stress relaxation, and on coarsening rates [12].

5. Conclusions

We have reported comparisons between surfactant (SDS) and protein (casein) foam properties, measured at different length scales. It is found that the microscopic origins of foam stability is quite different for SDS and casein foams. For surfactant solution, the repulsive interaction between the adsorbed layers provides the thin film and foam stability. The surface density is then an important parameter, and independent dynamic surface tension measurements are thus instructive. For casein foams, the mechanism of stability is related to the confinement of aggregates within the thin films, trapped there when bubbles come in contact (and not previously adsorbed). The film stability threshold appears to correspond to the percolation of these aggregates in the film. With this type of stabilization mechanism, which could be relevant for systems stabilized by other large proteins or solid particles, dynamic surface tension on single interfaces cannot be linked to macroscopic foamability. However, for both casein and SDS, it is found that there are always clear correlations between the stability of a single thin film and the one of the foam.

A new experimental setup for studying coarsening at constant liquid fraction (cell rotation, coupled to a light scattering measurement method) has been presented, allowing us to measure the time evolution of the mean bubble size inside a foam. It is then found that differences in thin film thickness can explain the ones seen on the coarsening rates. With this setup, more results are now being collected: other chemicals, gas, liquid fractions, or initial bubble size distribution.

Finally, though our results for mixtures of casein and SDS are preliminary, and as also reported from rheology experiments [12], it appears that the properties of such surfactant/protein solutions and foams seems to be rather different from the ones of their pure components, probably because of interactions both in the bulk and at the gas-liquid interfaces, which remains to be identified.

Acknowledgements

This work has been supported in part by the Centre National d'Etudes Spatiales (CNES) and the European Space Agency (ESA). The authors also thank the support from the Ministère de la Recherche (Réseau technologique RARE-SEA).

References

- [1] R.K. Prud'homme, S.A. Khan, *Foams, Theory, Measurements, and Applications*, Surfactant Science series, vol. 57, Marcel Dekker, New York, 1997.
- [2] D. Weaire, S. Hutzler, *The Physics of Foams*, Oxford University Press, New York, 1999.
- [3] V. Bergeron, *J. Phys. Cond. Matter* 11 (1999) R215, and references there in.
- [4] R. Von Klitzing, C. Stubenrauch, *J. Phys.: Cond. Matter* 15 (2003) R1197.
- [5] S.A. Koehler, S. Hilgenfeldt, E.R. Weeks, H. Stone, *J. Colloid Interface Sci.* 276 (2004) 439.
- [6] A. Saint-Jalmes, Y. Zhang, D. Langevin, *Eur. Phys. J. E* 15 (2004) 53.
- [7] E. Dickinson, *Colloids Surf. B* 20 (2001) 197.
- [8] E. Dickinson, *J. Chem. Soc., Faraday Trans.* 94 (1998) 1657.
- [9] A.H. Martin, K. Grolle, M.A. Bos, M.A. Cohen Stuart, T. van Vliet, *J. Colloid Interface Sci.* 254 (2002) 175.
- [10] G.B. Bantchev, D.K. Schwartz, *Langmuir* 19 (2003) 2673.
- [11] S. Cohen-Addad, R. Höhler, Y. Khidas, *Phys. Rev. Lett.* 93 (2004) 028302.
- [12] S. Marze, A. Saint-Jalmes, D. Langevin, *Proceedings of Eufoam 2004, Colloid Surf. A*, doi:10.1016/j.colsurfa.2005.01.014.
- [13] M. Meinders, W. Kloek, T. VanVliet, *Langmuir* 17 (2001) 3923.
- [14] W. Kloek, T. VanVliet, M. Meinders, *J. Colloid Interface Sci.* 237 (2001) 158.
- [15] A. Saint-Jalmes, M.U. Vera, D.J. Durian, *Eur. Phys. J. B* 12 (1999) 67.
- [16] S.H. Hilgenfeldt, S.A. Koehler, H.A. Stone, *Phys. Rev. Lett.* 86 (2001) 4704.
- [17] M.U. Vera, A. Saint-Jalmes, D.J. Durian, *Appl. Opt.* 40 (2001) 4210.
- [18] W.W. Mullins, *J. Appl. Phys.* 59 (1986) 1341.
- [19] J.A. Glazier, *Phys. Rev. Lett.* 70 (1993) 2170.
- [20] D.J. Durian, D.A. Weitz, D.J. Pine, *Phys. Rev. A* 44 (1991) 7902.
- [21] M.U. Vera, D.J. Durian, *Phys. Rev. Lett.* 88 (2002) 088304.
- [22] A. Saint-Jalmes, D. Langevin, *J. Phys.: Condens. Matter* 14 (2002) 9397.
- [23] V. Bergeron, D. Langevin, A. Asnacios, *Langmuir* 12 (1996) 1550.
- [24] L.G. Cascao-Pereira, C. Johansson, C.J. Radke, H.W. Blanch, *Langmuir* 19 (2003) 7503.
- [25] K. Koczko, A.D. Nikolov, D.T. Wasan, R.P. Borwankar, A. Gonsalves, *J. Colloid Interface Sci.* 178 (1996) 694.
- [26] V. Bergeron, *Langmuir* 13 (1997) 3474.
- [27] E. Dickinson, R. Ettelaie, B.S. Murray, Z. Du, *J. Colloid Interface Sci.* 252 (2002) 202.